

# Reduced Thermal Conductivity in Nanoengineered Rough Ge and GaAs Nanowires

Pierre N. Martin,<sup>\*,†,‡</sup> Zlatan Aksamija,<sup>†,‡</sup> Eric Pop<sup>\*,†,‡,§</sup> and Umberto Ravaioli<sup>†,‡</sup>

<sup>†</sup>Department of Electrical and Computer Engineering, <sup>‡</sup>Beckman Institute for Advanced Technology and Science, and <sup>§</sup>Micro- and Nano- Technology Laboratory, University of Illinois, Urbana–Champaign, Urbana, Illinois 61801

**ABSTRACT** We model and compare the thermal conductivity of rough semiconductor nanowires (NWs) of Si, Ge, and GaAs for thermoelectric devices. On the basis of full phonon dispersion relations, the effect of NW surface roughness on thermal conductivity is derived from perturbation theory and appears as an efficient way to scatter phonons in Si, Ge, and GaAs NWs with diameter  $D < 200$  nm. For small diameters and large root-mean-square roughness  $\Delta$ , thermal conductivity is limited by surface asperities and varies quadratically as  $(D/\Delta)^2$ . At room temperature, our model previously agreed with experimental observations of thermal conductivity down to  $2 \text{ W m}^{-1} \text{ K}^{-1}$  in rough 56 nm Si NWs with  $\Delta = 3$  nm. In comparison to Si, we predict here remarkably low thermal conductivity in Ge and GaAs NWs of  $0.1$  and  $0.4 \text{ W m}^{-1} \text{ K}^{-1}$ , respectively, at similar roughness and diameter.

**KEYWORDS** Nanowire, roughness, semiconductor, thermal, thermoelectricity

While semiconductor nanowires (NWs) have found viable applications in field effect transistors,<sup>1</sup> interconnects,<sup>2</sup> thermoelectrics,<sup>3–6</sup> and heterostructures,<sup>7,8</sup> scattering of carriers with the surface nevertheless limits transport in these devices, owing to their high surface-to-volume aspect ratio. Recent experimental and theoretical work<sup>4,9</sup> suggested that potentially high thermoelectric figures of merit  $ZT$  could be achieved by scattering phonons more effectively than electrons at the interfaces of rough NWs. In particular, thermal conductivity in Si NWs with etched rough edges was experimentally reduced by a factor of about 100 in comparison to bulk crystalline Si to nearly the value of amorphous Si, yielding a subsequent  $ZT \approx 0.6$  at room temperature.<sup>4</sup> Such nanostructured semiconductor materials present the advantage to enable energy efficient site-specific and on-demand cooling solutions,<sup>10,11</sup> and overcome the difficulties of integration into traditional microscale electronic devices.<sup>12,13</sup> With this respect, Ge or GaAs rough nanowires could provide convenient on-site energy conversion solutions for high current FET and optical applications based on Ge, GaAs, or strained Si on Ge technologies. In comparison to Si, Ge and GaAs have a naturally lower bulk thermal conductivity of  $\sim 59$  and  $\sim 42 \text{ W m}^{-1} \text{ K}^{-1}$ , respectively, higher bulk electrical conductivity,<sup>16,18,19</sup> and similar Seebeck coefficients, hence suggesting that rough Ge and GaAs NWs should have comparable thermoelectric efficiency as Si NWs. In previous  $\text{Bi}_2\text{Te}_3/\text{Sb}_2\text{Te}_3$  superlattice solutions, increases in  $ZT$  mainly originated from a reduction of the lattice thermal conductivity.<sup>14,15</sup>

In semiconductor NWs, charge carriers are naturally pushed away from the surface. Consequently, specular surface scattering is expected to reduce thermal conductivity in greater proportion than electrical conductivity and Seebeck coefficient. Hence, in rough Si NW, it was experimentally shown that the thermoelectric power factor remains high despite reduction of thermal conductivity.<sup>4</sup> In Ge and GaAs rough NWs, under the assumption that the power factor remains similarly unchanged by surface asperities, low thermal conductivity could have interesting repercussions on enhanced thermoelectric efficiency. In order to explore possible designs of thermoelectric NW coolers or generators, the present work theoretically addresses the trade-offs between different scattering mechanisms in Si, Ge, and GaAs necessary to achieve necessary to achieve low thermal conductivities through surface nanostructuring.

It is expected that vibrations of the crystal lattice interfere with the spatial fluctuations of the NW boundaries. Nevertheless, most of the work in phonon transport only accounts for surface roughness scattering by a constant fitting parameter which reflects an average probability of diffuse scattering at the NW surface. We recently proposed<sup>9</sup> a perturbative approach to phonon–surface roughness scattering, where a matrix element is derived for such interactions. This model has shown excellent agreement with experimental observations on rough Si NWs with diameter below 50 nm where the effect of surface roughness is the strongest. Here, we use our modeling platform to investigate the case of GaAs and Ge NWs. The roughness of a surface is generally quantified by its root mean square (rms) height  $\Delta$  and autocorrelation length  $L$ . The present model accounts for the variation of NW thermal conductivity with the experimentally observable  $\Delta$ ,  $L$ , and the phonon angular frequency  $\omega$ . In order to ac-

\* To whom correspondence should be addressed. pmartin7@illinois.edu.

Received for review: 08/20/2009

Published on Web: 03/11/2010



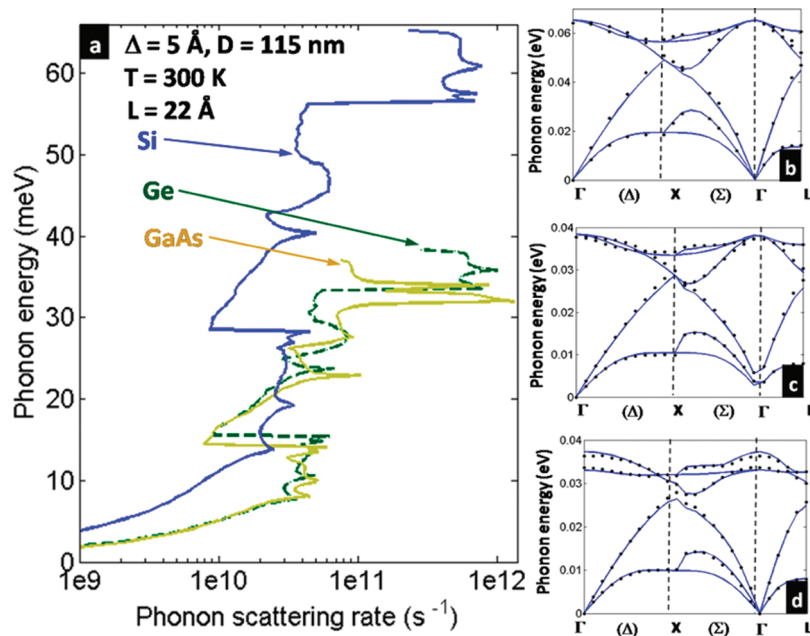


FIGURE 1. (a) Phonon–surface roughness scattering rates computed at room temperature in Si, Ge, GaAs. (b), (c), and (d) Computed full phonon branches in the first Brillouin zone of Si, Ge, and GaAs, respectively. Dots are extracted from experimental observations<sup>25,26</sup> for comparison.

curately capture the effect of phonon frequency on surface roughness scattering rates, a full-phonon dispersion relation is used for Ge and GaAs (Figure 1). For the first time, we introduce a parabolic estimation of Ge and GaAs phonon dispersion relation in order to speed up full branch computations, which nevertheless reflect both experimental and computed branches within a 0.8% error margin. This approach accurately predicts phonon–surface roughness scattering to contribute to the reduction of thermal conductivity by a factor  $(D/\Delta)^2\omega^{-2}$  where  $D$  is the NW diameter. In addition, the quality of thermoelectric devices is measured by the dimensionless figure of merit  $ZT = (S^2\sigma/\kappa)T$ , where  $S$  is the Seebeck coefficient,  $T$  the temperature,  $\sigma$  the electrical conductivity, and  $\kappa$  the thermal conductivity. With this respect, a standard approach to achieve performance is to design a “phonon glass–electron crystal”, with high electron mobility and poor thermal conductivity. Among thermally resistive mechanisms in a semiconductor crystal, scattering of phonons by isotopes<sup>16</sup> or in three-phonon anharmonic decays<sup>20</sup> is also of considerable importance.

Our model assumes that no phonon is emitted to the surrounding environment. This condition reflects the case where NWs are wrapped in a medium of considerably different  $\kappa$ , as it is for semiconductor NWs wrapped in oxide or suspended in vacuum. Despite neglecting effects of natural oxide layers present in the case of suspended NW, the assumption above yielded accurate predictions in previous Si models.<sup>9</sup> In addition, considering higher order phonon decays in such peripheral oxide layers of poor  $\kappa$ <sup>17</sup> will only serve to reduce the exceptionally low Ge and GaAs NW thermal conductivities reported here. While propagating along wires of diameter  $D < 500$  nm, phonons scatter from

a series of constrictions along the transport direction which result from the surface asperities and are reflected by a perturbed Hamiltonian  $H'$  of the system. The interface roughness is treated as a space varying dilatation  $\delta(r)$  of the wire, whose autocorrelation function is assumed to be exponential  $\Delta(r) = \Delta\exp(-r/L)$ . Following the derivation of Klemens,<sup>20</sup> the matrix element for a perturbation due to a space varying dilatation reflects the transitions of phonons from a state of momentum  $\mathbf{k}$  to  $\mathbf{k}'$  such as

$$|\langle \mathbf{k} | H' | \mathbf{k}' \rangle|^2 = \frac{4\gamma^2}{3V_{\text{ol}}}\omega^2(\langle n' \rangle + 1)\Delta(\mathbf{k} - \mathbf{k}') \quad (1)$$

where  $V_{\text{ol}}$  is the volume of the device,  $\gamma$  is Grüneisen’s parameter,  $\omega$  is the angular frequency of the incident phonon, and  $\Delta(\mathbf{q}) = \pi\Delta^2L^2\exp(-L^2\mathbf{q}^2/4)$  is the roughness power spectrum associated with  $\Delta(r)$ . Close to equilibrium, the occupation of the destination phonon branch  $\langle n' \rangle$  is given by the Bose–Einstein distribution and reflects the temperature dependence of the model  $\langle n' \rangle = (\exp(\hbar\omega/k_B T) - 1)^{-1}$ . The probability of transitions from  $\mathbf{k}$  to  $\mathbf{k}'$  due to surface roughness is directly proportional to the matrix element derived above. As a consequence of the  $\omega^2$  factor, low-frequency phonons experience little thermal resistance from surface asperities. In addition, the dependence on the autocorrelation length  $L$ , which represents the average width of roughness peaks, shows that smoothly varying surfaces favor scattering events of the specular type.

TABLE 1. Summary of the Scattering Processes and Associated Parameters Used in the Derivation of Ge and Ga as Thermal Conductivity<sup>a</sup>

	GaAs <sup>27</sup>	Ge <sup>16</sup>
phonon–phonon:		
Umklapp	$B_{\lambda}T^5(\hbar\omega/k_B T)^2 \exp(-\theta_{\lambda}/T)$	$B_{\lambda}T^5(\hbar\omega/k_B T)^2 \exp(-\theta_{\lambda}/T)$
normal: transverse	$D_t T^5(\hbar\omega/k_B T)$	$D_t T^5(\hbar\omega/k_B T)$
normal: longitudinal	$D_l T^5(\hbar\omega/k_B T)^2$	$D_l T^5(\hbar\omega/k_B T)^2$
phonon disp. (100)	$\omega(q) = \omega_0 + v_{\lambda}q + c_{\lambda}q^2$	$\omega(q) = \omega_0 + v_{\lambda}q + c_{\lambda}q^2$
$B_i$ (K <sup>-5</sup> /s)	$8.252 \times 10^5$	$6.119 \times 10^5$
$\theta_i$ (K)	40.791	58.06
$B_l$ (K <sup>-5</sup> /s)	$3.268 \times 10^{-3}$	$2.80 \times 10^{-3}$
$\theta_l$ (K)	22.764	221.337
$D_t$ (K <sup>-4</sup> /s)	$4.17 \times 10^{-4}$	$9.26 \times 10^{-4}$
$D_l$ (K <sup>-3</sup> /s)	0.4814	42.38
$A$ (s <sup>2</sup> )	$0.466 \times 10^{-44}$	$1.78 \times 10^{-44}$
$v_{ta}, v_{la}$ (m/s)	3566.9, 5320.6	3616.7, 5342
$v_{to}, v_{lo}$ (m/s)	-50.84, 155.82	-960.41, 294.97
$c_{ta}, c_{la}$ (m <sup>2</sup> /s)	$-2.017 \times 10^{-7}, -1.314 \times 10^{-7}$	$-2.09 \times 10^{-7}, -1.10 \times 10^{-7}$
$c_{to}, c_{lo}$ (m <sup>2</sup> /s)	$2.29 \times 10^{-8}, -9.84 \times 10^{-8}$	$4.134 \times 10^{-8}, -1.24 \times 10^{-7}$

<sup>a</sup> Si properties are listed in Martin et al.<sup>9</sup>

We use a Gilat–Raubenheimer (GR)<sup>21,22</sup> scheme to compute the surface roughness scattering rate integrals in Si, Ge, and GaAs (see Figure 1a)

$$\tau_{i,j}^{-1}(E) = \frac{2\pi}{\hbar N_i(E)} \int_{E'=E_i} \frac{|\langle \mathbf{k} | H' | \mathbf{k}' \rangle|^2}{\nabla_{\mathbf{k}} E'(\mathbf{k}')} dS \quad (2)$$

where  $\tau_{i,j}^{-1}$  is the transition rate from phonon branch  $i$  to  $j$  due to surface roughness,  $N_i(E)$  is the branch phonon density of state, and  $E'(\mathbf{k})$  is the phonon dispersion relation on the destination branch  $j$ . In order to account for the frequency dependence of the phonon–surface roughness interference process, full dispersion relations are used, which are obtained from an adiabatic bond charge model, and approximate the dispersion relations observed in Si, Ge, and GaAs<sup>25,26</sup> with a 1–2.5% error (Figure 1b–d). The GR scheme approximates surface integrals on the first Brillouin zone (FBZ) discretized over  $40 \times 40 \times 40$  cubes, which achieves sufficient accuracy in the 10–350 K range.<sup>23</sup> While the Gaussian approximation may be put at fault in the strong roughness limit where  $\Delta/L > 1$ , the effect of the  $L^2$  term tends to average out the contribution of  $L$ . We noticed only little deviation of the predicted thermal conductivity in the strong roughness limit and consistently used a value of  $L = 22 \text{ \AA}$  which provides a good fit in all cases.

The latter surface roughness scattering rate is added to the total scattering rate by Mathiessen’s rule. Subsequently, we compute thermal conductivity with Holland’s formalism<sup>27</sup>

$$\kappa = \frac{\hbar^2}{6\pi^2 k_B T^2} \sum_i \int \omega_i^4(q) \tau_i^{\text{tot}}(q) \frac{\exp(\hbar\omega_i/k_B T)}{(\exp(\hbar\omega_i/k_B T) - 1)^2} dq \quad (3)$$

where  $i$  goes over all incident transverse and longitudinal branches, and the wave vector  $q$  models conduction in the

NW along the  $\Gamma-(\Delta)-X$  direction. For additional computational speed, an analytic expression<sup>24</sup> is used for the phonon branches in the propagation direction where

$$\omega(q) = \omega_0 + v_{\lambda}q + c_{\lambda}q^2 \quad (4)$$

The parabolic parameters are obtained in Ge and GaAs from a best fit to experimental observation<sup>25,26</sup> and reported in Table 1. In addition to surface roughness scattering, computations of  $\kappa$  include boundary, isotope, three phonon Umklapp, and normal decay processes. Parametric laws are used for the latter rates, which are fitted to best reflect experimental bulk  $\kappa$  values<sup>16,27</sup> as described in Table 1 and represented in Figure 2 in the 10–400 K temperature range. In the case of Si, the parameters of Martin et al.<sup>9</sup> are used for their good fit with experimental observations on Si NW. Bulk boundary scattering is fixed to the value reported from experimental observations.<sup>16,27</sup> The impurity scattering rate varies as  $A\omega^4$ , where  $A$  reflects isotope concentrations.  $A$  is not fitted, as we chose isotope concentrations of group IV semiconductors to match their natural occurrence, with 92.2% of <sup>28</sup>Si, and noticeably only 36.5% of <sup>74</sup>Ge.<sup>16</sup> As a result of its heavier atomic mass and high natural isotope concentration, Ge shows lower  $\kappa$  throughout all simulations (Figure 3 and Figure 4).

Subsequently,  $\kappa$  is computed for Ge and GaAs NWs of various diameters and  $\Delta$  (Figure 2). Although no reliable data on the roughness of small wires are available yet, recent studies have reported roughness rms ranging from 3 Å for smooth vapor–liquid solid (VLS) grown NW to 5 nm in the case of extremely rough etched NWs.<sup>4</sup> It is noticeable that the effect of reduced dimensions is stronger in rough NWs in comparison to the ideally smooth case. In Figure 3 and Figure 4, NW thermal conductivity is predicted to decrease in rough wires (high rms  $\Delta$ ). The  $(D/\Delta)^2$  behavior is apparent in thin NWs of diameter  $D < 115 \text{ nm}$ , showing that phonon–surface roughness scattering is the dominant resis-

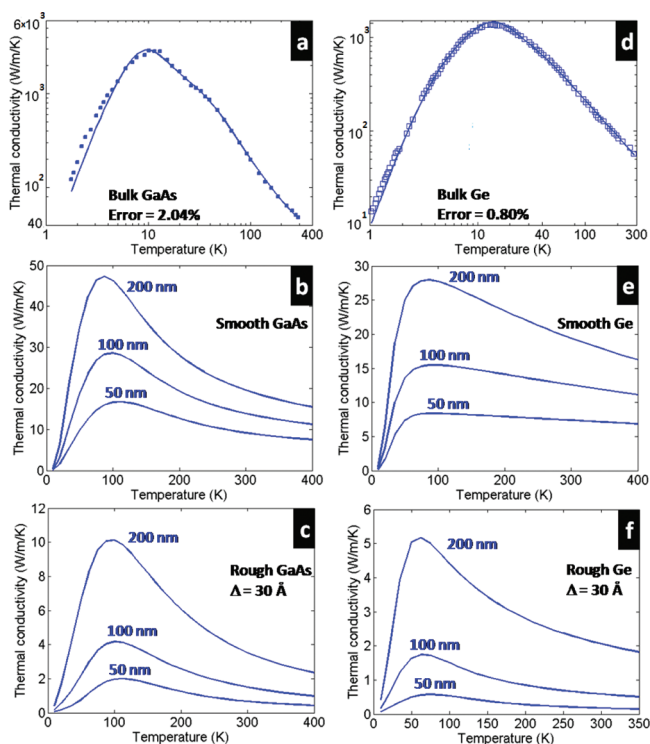


FIGURE 2. Parametric fit of the scattering rates on experimental bulk thermal conductivity (squares) of (a) GaAs<sup>27</sup> and (d) Ge.<sup>16</sup> Diameter dependence of NW thermal conductivity in (b) ideally smooth and (c) rough ( $\Delta = 30 \text{ \AA}$ ,  $L = 22 \text{ \AA}$ ) GaAs NW and (e) ideally smooth and (f) rough ( $\Delta = 30 \text{ \AA}$ ,  $L = 22 \text{ \AA}$ ) Ge NW.

tive process in this case. For intermediate diameters ( $D/\Delta \approx 100$  for Ge and GaAs, 50 for Si), the linear dependence in the diameter suggests that phonons dominantly decay from classical boundary scattering  $\tau_B^{-1}(q) = v_s/D$ , with  $v_s$  the average speed of sound in each branch. For wider  $D$ ,  $\kappa$  converges to its bulk value.

Low NW thermal conductivity results from the combination of all concurrent interference processes mentioned above: isotope, impurity, Umklapp, and surface. While impurities tend to also reduce mobility, isotope scattering limits thermal conductivity and keeps electrical conductivity unchanged. At temperatures of 300 K and above, where the conduction is primarily limited by Umklapp scattering, the

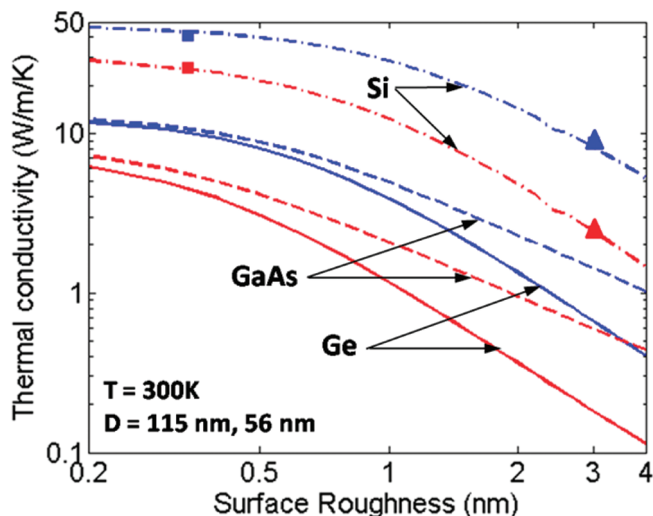


FIGURE 4. Effect of roughness rms on thermal conductivity of Si, Ge, and GaAs NW with diameters of 115 nm (upper curve) and 56 nm (lower curve).  $L = 22 \text{ \AA}$  throughout.

most sensitivity to isotope and surface scattering is obtained in NWs fabricated from materials that have naturally low bulk Umklapp scattering rates. In particular, the effect of artificially high  $\Delta$  and low  $D$  decreases thermal conductivity below  $1 \text{ W m}^{-1} \text{ K}^{-1}$  in Ge and GaAs NWs of diameter  $D = 56 \text{ nm}$ . At this scale, fabrication of rough etched NWs is feasible,<sup>4</sup> and the perturbative approach holds validity as the ratio  $\Delta/D$  is only of a few percent, showing good agreement with experimental results (Figure 4). Noticeably, the best fit for the natural Ge sample shows strong isotope and weak Umklapp scattering. As a result, Ge experiences the starkest influence from surface roughness scattering at high temperatures, with an extraordinarily low  $\kappa \approx 0.1 \text{ W m}^{-1} \text{ K}^{-1}$  at  $D = 56 \text{ nm}$  and  $\Delta = 4 \text{ nm}$ . GaAs, with respect to all phonon decay processes, experiences the strongest Umklapp scattering rate, and the effect of surface roughness remains moderate in comparison to Si and Ge (Figure 4). In the case of silicon, the experimental observations of Hochbaum et al.<sup>4</sup> clearly show that enhancement of the thermoelectric figure of merit  $ZT = S^2\sigma/\kappa T$  is due to a strong reduction by a factor 100 of the thermal conductivity, while the factor  $S^2$  remains constant under the effect of surface roughness at

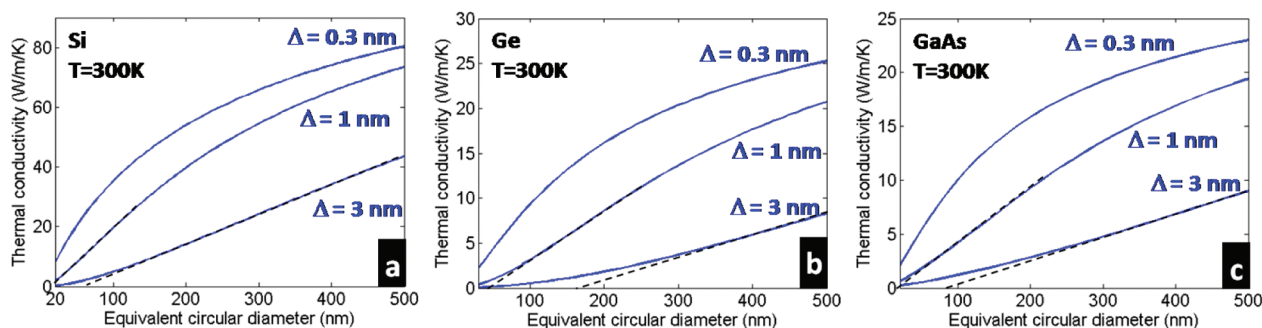


FIGURE 3. Effect of NW diameter on thermal conductivity for varying roughness rms in (a) Si (after Martin et al.<sup>9</sup> for  $D = 20\text{--}116 \text{ nm}$ ), (b) Ge, and (c) GaAs.  $L = 22 \text{ \AA}$  throughout.

300 K in comparison to bulk values. We expect GaAs and Ge to behave quantitatively the same and predict in this paper that surface roughness will reduce GaAs and Ge thermal conductivity by factors of 7 and 60, respectively (Figure 4), with an expected increase of thermoelectric figure of merit in the same proportions. In addition, earlier modeling<sup>6</sup> of the variation of the power factor  $S^2\sigma$  and thermal conductivity with the diameter of smooth NWs, based on solutions to the Boltzmann transport equation, revealed that improvement of  $ZT$  in thermoelectric NWs is due to a reduction of thermal conductivity rather than the power factor. Indeed, improvement of the power factor is theoretically limited since the acoustic phonon–electron scattering drastically increases when the diameter of the NW is reduced.<sup>6,8</sup> Nevertheless, in order to obtain accurate expectations for the figure of merit, the effect of surface roughness needs to be included into estimates of the power factor.<sup>2</sup> The authors are currently unaware of such models and therefore recommend further investigation in this direction. Our model eventually predicts weak interference between low energy phonons and surface asperities. Consequently, we notice very little variation of thermal conductivity with respect to the roughness rms at temperatures below 100 K.

In summary, we modeled thermal properties of artificially rough Si, Ge, and GaAs NWs based on a perturbative treatment of the interaction between lattice vibrations and surface asperities. This approach, based on a full phonon dispersion in each material, accurately accounts for the frequency dependence of phonon scattering processes resulting from surface roughness, isotope, boundary, and anharmonic decays. Our model predicts  $\kappa \propto (D/\Delta)^2$  for thin NWs, yielding remarkably low thermal conductivity in rough etched Ge and GaAs NWs of diameter  $D < 115$  nm, thus revealing those materials as potential candidates for efficient site-specific, on-demand, integrated thermoelectric energy conversion solutions. For the same diameter and roughness rms, GaAs and Ge NWs are expected to have approximately 5 times and 10 times lower thermal conductivity than Si NWs, respectively, at room temperature. Similar scattering mechanisms nevertheless limit electron mobility, making it necessary to model charge transport in order to find optimal thermoelectric figures of merit  $ZT$ . In this scope, it is notice-

able that isotopes have no influence on electronic conduction, and surface roughness may only have limited impact at low  $D$  where electrons tend to be pushed away from the interface. Hence, those two factors are expected to be significant design parameters in the engineering of efficient semiconductor NW thermoelectric devices.

**Acknowledgment.** This work was supported in part by the DARPA through the IMPACT Center for Advancement of MEMS/NEMS VLSI Grant No. HR0011-06-1-0046 (P.M.), the DOE Computational Science Graduate Program of the OSNNSA under Contract DE-FG02-97ER25308 (Z.A.), and the Nanoelectronics Research Initiative (NRI) SWAN center (E.P.).

## REFERENCES AND NOTES

- (1) Singhan, N.; Agarwal, A.; Bera, L.; et al. *IEEE Electron Device Lett.* **2006**, *27*, 383.
- (2) Steinhogel, W. *Appl. Phys. Lett.* **2006**, *97*, 023706.
- (3) Li, D.; et al. *Appl. Phys. Lett.* **2003**, *83*, 2934.
- (4) Hochbaum, A.; Chen, R.; Delgado, R.; et al. *Nature* **2008**, *451*, 163.
- (5) Ramayya, E.; Vasileska, D.; Goodnick, S.; et al. *IEEE Conf. Nanotechnol.*, *8th* **2008**, 339.
- (6) Mingo, N. *Appl. Phys. Lett.* **2004**, *84*, 2652.
- (7) Dames, C.; Chen, G. *J. Appl. Phys.* **2004**, *95*, 682.
- (8) Broido, D.; Reinecke, T. *Phys. Rev. B* **2001**, *64*, 045324.
- (9) Martin, P.; Aksamija, Z.; Pop, E.; Ravaoli, U. *Phys. Rev Lett.* **2009**, *102*, 125503.
- (10) Mahajan, R.; Chiu, C.; Chrysler, G. *Proc. IEEE* **2006**, *94*, 1476.
- (11) Prasher, R.; et al. *Intel Technol. J.* **2005**, *9*, 285.
- (12) Majumdar, A. *Nat. Nanotechnol.* **2009**, *4*, 214.
- (13) Chowdury, I.; Prasher, R.; et al. *Nat. Nanotechnol.* **2009**, *4*, 235.
- (14) Hsu, K.; et al. *Science* **2004**, *303*, 818.
- (15) Harman, T.; Taylor, P.; Walsh, M.; et al. *Science* **2002**, *297*, 2229.
- (16) Asen-Palmer, M.; et al. *Phys. Rev. B* **1997**, *56*, 9431.
- (17) Li, S.; Cahill, D.; Allen, H. *Phys. Rev. B* **1995**, *52*, 253.
- (18) Baraman, S.; Srivastava, G. *Phys. Rev. B* **2006**, *73*, 205308.
- (19) Fon, W.; Schwab, K.; Worlock, J.; Roukes, M. *Phys. Rev. B* **2002**, *66*, 045302.
- (20) Klemens, P. *Solid State Phys.* **1958**, *7*, 1.
- (21) Gilat, G.; Raubenheimer, L. *Phys. Rev.* **1966**, *144*, 390.
- (22) Weber, W. *Phys. Rev. B* **1977**, *15*, 4789.
- (23) Aksamija Z. Ravaoli U. Energy conservation in collisional broadening. *Simulation of Semiconductor Processes and Devices*; Springer: Vienna, 2007; p 73.
- (24) Pop, E.; et al. *J. Appl. Phys.* **2004**, *96*, 4998.
- (25) Strausch, D.; Dorner, B. *J. Phys.: Condens. Matter* **1990**, *2*, 1457.
- (26) Nilsson, G.; Nelin, G. *Phys. Rev. B* **1972**, *6*, 3777.
- (27) Holland, M. *Phys. Rev.* **1964**, *134*, 471.